

MRI-based cerebrovascular plaque segmentation using a new hybrid snake

B. Das¹, P. K. Saha¹, R. Wolf¹, H. K. Song¹, A. C. Wright¹, E. R. Mohler², F. W. Wehrli¹

¹Department of Radiology, University of Pennsylvania, Philadelphia, PA, United States, ²Presbyterian Medical Center, Philadelphia, PA, United States

SYNOPSIS: Atherosclerosis is a vessel wall disease occurring at the aorta, coronary, peripheral, intra- and extra-cerebral arteries, leading to lipid-laden plaques that may eventually impair cerebral blood flow. Rupture of atherosclerotic plaques in the carotid arteries can form emboli that can obstruct cerebral vessels leading to transient ischemic attacks or, in the worst case, stroke, one of the leading causes of death and disability. Here, we present a hybrid snake algorithm for computer-assisted vessel wall segmentation and quantification of disease burden. We further evaluate its performance on patient data on the basis of double inversion black-blood MR images.

INTRODUCTION: Atherosclerosis is a vessel wall disease occurring at the aorta, coronary, peripheral, intra- and extra-cerebral arteries, leading to lipid-laden plaques that may eventually impair cerebral blood flow¹. Rupture of atherosclerotic plaques in the carotid arteries can form emboli that can obstruct cerebral vessels leading to transient ischemic attacks or, in the worst case, stroke, one of the leading causes of death and disability². Although the risk of a lesion to produce symptoms does not only depend on the size of the constriction, quantification of lesion burden is important as a means to evaluate the effect of lipid-lowering drugs. Therefore, a robust computer-assisted method for vessel boundary segmentation with minimal user intervention is highly desirable. Here, we present a hybrid snake algorithm for computer-assisted vessel wall segmentation and quantification of disease burden. We further evaluate its performance on MR images of the neck in patients with occlusive disease.

METHOD: Snake⁴ is deformable spline that is governed by its own elastic properties and various image- and user-guided features so as to snap to the target object boundary. The limitations of conventional snakes is their frequent failure to cope with weak boundaries as they are common in MR vessel wall imaging, in particular, as far as the delineation of the outer wall is concerned. Here, we introduce a class-uncertainty-tailored adaptive force that optimally uses the expected values and the chaos in MR signal to stop undesired leakage. Further, we present a new hybrid force-field model to maximally utilize the vector information of image features. In addition, the hybrid snake (HS) has been augmented by three new features: (1) *Forbidden zone*: A distance-transform-guided forbidden zone is defined after initial lumen delineation to prevent the interference of its strong boundary during outer vessel wall segmentation. (2) *Smooth wire deformation*: A Gaussian-weighted arc representation of local control points is formulated for a better utilization of the smoothness property of outer vessel walls. (3) *Arc-based landmark*: A new arc-based landmark specification is introduced for efficient user interaction reducing inflexion artifacts near landmarks. Cross-sectional PD-weighted MR images (voxel size: 0.47x0.47x2.0 mm³, FOV: 120x120x32 mm³) of the neck displaying atherosclerotic lesions of the carotid arteries were acquired at 1.5T (Siemens Sonata) using a double inversion black-blood pulse sequence³. Both accuracy and reproducibility of the HS were evaluated using MR data sets of 10 patients who were indicated for endarterectomy at the authors' institution. Since no ground truth exists, the method's performance was evaluated against results from manual segmentation by two expert radiologists (R1,R2). Lumen (L) and vessel wall (V) areas and mean vessel wall thickness (VT) were separately computed for HS, R1, and R2 and the deviations of the HS measures from those of R1 and R2 were analyzed. To assess reproducibility, each patient MR data set was segmented thrice (T1,T2,T3) using HS by the same user at intervals of 15 days. Similar measures as used for accuracy were computed for reproducibility but between two HS segmentations at different time points.

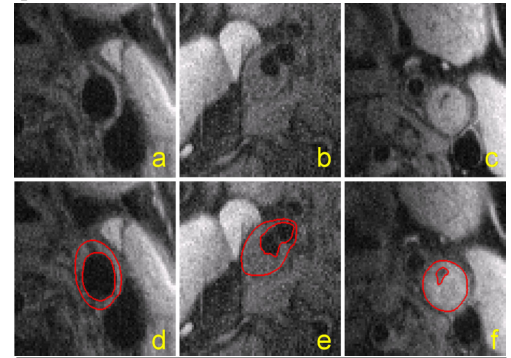


Figure 1: HS-based lumen and vessel segmentation on three patient MR image slices with various levels of atherosclerotic plaques.

RESULTS AND DISCUSSION: Examples of application of the HS are illustrated in Figure 1. Figure 2a shows the results of the performance analysis comparing vessel wall area derived by HS methods to those computed from manual segmentations of lumen and vessel outer boundaries (**R1**: $r^2_V=0.92$, $r^2_L=0.98$, $r^2_{VT}=0.89$; **R2**: $r^2_V=0.88$, $r^2_L=0.96$, $r^2_{VT}=0.86$). Also, inter-observer segmentation variability of manual segmentation between R1 and R2 were estimated for the same patient data sets. The results (**R1 & R2**, $r^2_V=0.77$, $r^2_L=0.97$, $r^2_{VT}=0.76$) were inferior to their individual comparisons with the HS method. These results suggest that the segmentations by the HS method is statistically in between the two experts' segmentations. Figure 2b illustrates the results of the reproducibility experiment (**T1&T2**: $r^2_V=0.95$, $r^2_L=0.99$, $r^2_{VT}=0.90$; **T1&T3**: $r^2_V=0.98$, $r^2_L=0.99$, $r^2_{VT}=0.90$). The results suggest that L and V are highly reproducible while that for VT is moderate. The lower reproducibility for VT is attributed to the small mean vessel wall thickness. The variability in segmentation of the two boundaries (L&V) magnify the error in thickness measurement. Both accuracy and reproducibility of the method suggest its potential use for monitoring the response to treatment.

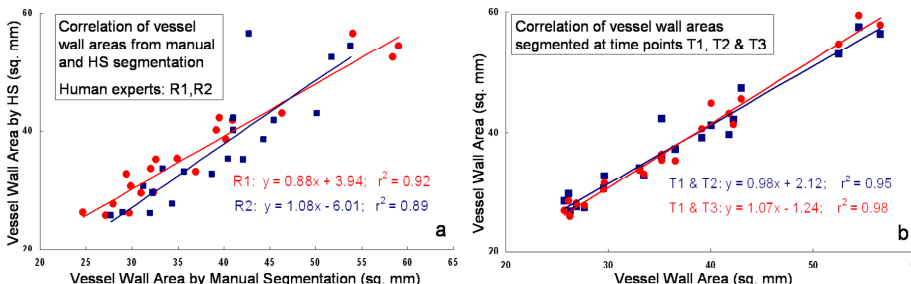


Figure 2: Accuracy and reproducibility of the HS method for 10 patient MR data sets: (a) accuracy: correlations of vessel wall area obtained by the HS method versus that obtained by two experts (R1,R2); (b) reproducibility: correlations of vessel wall areas obtained by the HS method applied to the same MR data at three time points 15 days apart.

REFERENCES: [1] R. Ross, *The New England J Med* 340:115-126, 1999. [2] R. Ross, *Nature*, 362:801-809, 1993. [3] R.R. Edelman *et al*, *Radiology* 181: 655-660, 1991. [4] M. Kass *et al.*, *Int J Comp Vis* 1:321-331, 1988. [5] B. Das *et al.*, *Proc. SPIE Med Imag*, 5370:369-380, 2004.

ACKNOWLEDGEMENT: This work is supported by NIH R01-HL68908.